Chapter 5

Energy Management System for Smart Buildings under FDI Attack-Centralized Approach

5.1 Introduction

In previous chapter we have discussed the multiple smart building Energy Management system (EMS) without considering power exchange capability among the buildings. In this chapter, EMS for multiple smart building with power exchange capability have been developed.

Smart homes are end-users of power grids, and they are essential components of the smart grid infrastructure. Smart home appliance scheduling techniques play a significant role in smart home energy management systems as they are responsible for energy consumption. Multiple smart building energy management systems (MSBEMS) specifically aims to reduce dependency on the main utility as they can trade power among themselves. In this way, the consumer's average energy cost is reduced, and the energy load balance of the power grid is maintained. Electricity pricing scheme from the utility side guides the energy consumption of the consumers. The utility also provides its consumer with a Demand Response (DR) program for proper energy usage at different time intervals. Renewable Energy Sources (RESs) such as roof-top wind turbine and solar PV panels are installed in residential smart buildings. Also, to manage the intermittent behaviour of wind and solar system, smart homes may use Battery Storage Systems (BSSs) in residen-

tial buildings. For the effective operation of MSBEMS, a secure and intelligent system incorporating Information Technology (IT) and Advanced Metering Infrastructure (AMI) is required.

The communication infrastructure requires two main components, the Home Area Network (HAN) and the Utility Network (UN), to implement scheduling of smart home devices in MSBEMS. The said components need to be integrated with ICT along with intelligent technologies, advanced metering infrastructures, and different home area networks (such as WiFi, 802.11, and ZigBee) and utility network (such as WiMAX, IEEE 802.16E, and broadband PLC). This system is prone to cyber-attacks. Energy management under cyber-attack will be one of the important issues in the current power system scenario.

A multiple smart building energy management system with detection and defense strategy against FDI attack is proposed. In addition, the optimal scheduling of smart home appliances, taking into account the capability of power exchange between smart buildings, is proposed to reduce operating costs. In the present work, energy cost minimization with FDI attack constraints in the scheduling process are considered. The major contributions of this chapter can be summarized as follows.

- A resilient scheduling strategy for interconnected multiple smart buildings, with power import and export capabilities, is proposed to eliminate the effect of FDI attack.

- The FDI attack detection is achieved using the difference in forecasted and actual bills also the same information is used to make the resilient scheduling. The forecasted bill is obtained using Gaussian process regression model.

5.2 System Architecture

Energy management of multiple smart buildings is considered in this chapter. The basic architecture of the system is shown in Figure 5.1. This architecture consists of three interconnected Smart Buildings (SBs), and each smart building comprises four SHs. Each smart building is equipped with DERs such as rooftop solar PV, wind turbines, battery storage systems (BSSs) and, Combine Heat and Power (CHP) generators. Residential

consumers use RESs such as rooftop solar PV and small wind turbines to reduce their energy cost and dependence on the main utility. Smart home users use a BSSs to improve the reliability of supply in the presence of uncertainties of solar and wind power generation. The MSBEMS-based system is proposed to manage domestic loads and battery operating

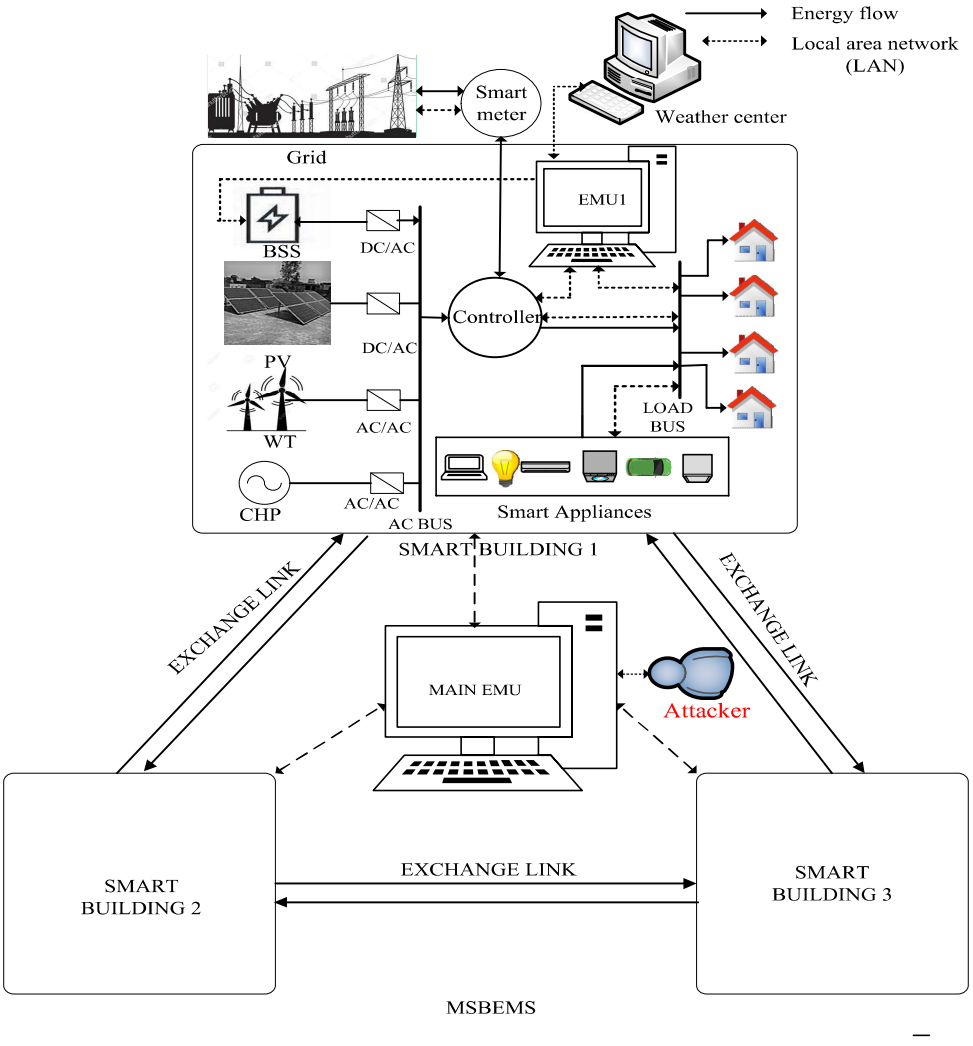

Figure 5.1: Architecture of MSBEMS

mode (charging, discharging) so that energy production by RESs can be used effectively. Each smart home includes a variety of smart appliances such as washing machine (WM), dish washer (DW), tumble dryer, cooker hob, microwave, cooker oven, lighting bulb, laptop, desktop, vacuum cleaner, refrigerator and electric vehicle (EV). Each smart building is equipped with its local Energy Management Unit (EMU) which is a computer-aided device used by the operator to monitor, control, optimize generation, and schedule home

appliances. Each smart building is also equipped with a smart controller connected to all DERs, smart grids, and smart appliance. This smart controller switches smart appliance and DERs in the smart building. All the EMUs of smart building are connected to the main EMU, which manages the total energy of the MSBEMS and checks whether it is possible to import or export electricity between buildings. MSBEMS can obtain information about the Maximum Demand Limit (MDL) and power export limit (PEL) as well as the change in power price from the grid through the local area network.

5.3 Problem Formulation

5.3.1 Energy Cost Minimization

In this chapter, the objective is to reduce energy cost by Real-time Pricing (RTP) based scheduling of smart home appliances. Different types of constraints employed in the current work are related to consumers' requirement as reflected in terms of operation and duration of operation of equipment, RES power availability, battery storage constraints, CHP generator constraints and MDL.

As some loads such as laptops, televisions, electric bulbs, desktops, fans depend on the consumers activity, thus EMU does not have the authority to control these type of loads. When total power consumption breaches the MDL, a warning signal is generated by the EMU. However, EMU has the authority to control the Temperature Dependent Loads (TDLs) such as refrigerators and air conditioners considering their temperature settings. Therefore, the EMU has the flexibility to turn ON/OFF these loads as described in the Chapter 2.

To reduce the energy cost of the consumer, the EMU tries to shift the load from peak hours to the off-peak hours. Also, SBs exchange power at a rate lower than the utility selling price but higher than the utility purchase price according to their surplus and deficit status. For example, if one SB has a lower power demand than the generated power, and if the power demand of other SBs is greater than the generated power, then they exchange power. Therefore, the function of MSBEMS is to make effective use of RESs and CHP generation and maintain power demand below MDL. To reduce electricity bills and reduce dependency on utility, the scheduling of loads and power exchange capability are indispensable. The purpose of this Chapter is to propose strategy to reduce energy

costs in smart building architectures considering the CHP generator natural gas price and battery maintenance costs. Cyber-attack detection and defence strategy have also been incorporated in the formulation. Thus, the objective function can be formulated as follows,

$$Obj = min \sum_{b} C(b), \tag{5.1}$$

where,

$$C(b) = \sum_{t} [P^{dis}(b,t) \times \lambda_{bmc} + P^{chp}(b,t) \times \lambda_g + P^{gimp}(b,t) \times \lambda(t) - P^{gexp}(b,t) \times \lambda_x(t) + \Big(\sum_{n,b \neq n} P_{bim}(b,n,t) - \sum_{n,b \neq n} P_{bex}(b,n,t) \Big) \times \lambda_x(t)]. \tag{5.2}$$

Here, $C(b)$ and $P^{dis}(b,t)$ are respectively the energy cost and baterry discharging power of b^{th} smart building at time interval t, λ_{bmc} is the battery maintenance cost, $P^{chp}(b,t)$ is the CHP generator power. λ_g is natural gas price, $P^{gimp}(b,t)$ and $P^{gexp}(b,t)$ are the grid import and export powers respectively, $\lambda(t)$ is the forecasted electricity price, $\lambda_x(t)$ is the export price, P_{bim} and P_{bex} are the building import and export powers respectively.

The time and power consumption of appliance, a_i, should satisfy the following constraints.

$$\sum_{t} S_{a_i}(t) = T_{min,a_i}. \tag{5.3}$$

$$P_{a_i}(t) = \sum_{t} S_{a_i}(t) \times P_{rated,a_i}. \tag{5.4}$$

Here, T_{min,a_i}, S_{a_i} and P_{rated,a_i} are respectively the minimum ON time, binary variable and power ratings of a_i^{th} appliance. Here, $a_i \in \{a_u, a_s, a_{td}\}$ and a_u, a_s and a_{td} are the indices of UNLs, SLs and TDLs respectively. $P_{a_i}(t)$ is the power consumption of a_i^{th} appliance at time interval t.

Smart appliances operate according to their start-time and end-time. The status, $S_{a_i}(t)$, of a_i^{th} appliance can be described as follows.

$$S_{a_i}(t) = \begin{cases} 1, & \text{if ON} \\ 0, & \text{otherwise.} \end{cases} \tag{5.5}$$

Power and heat demands of each SH are described by Eq.(5.6) and Eq.(5.7) respectively.

$$P_h(t) = \sum_{a_i \in (a_s, a_{td}, a_u)} P_{a_i}(t). \tag{5.6}$$

$$H_h(t) = \sum_i H_i(t). \tag{5.7}$$

Here, $P_h(t)$ and $H_h(t)$ are respectively power and heat demand of h^{th} smart home, and $H_i(t)$ is the heat required by i^{th} appliance.

The load demand and power balance equation of each SB without power exchange capability can be expressed as,

$$P_b(t) = \sum_h P_h(t), \tag{5.8}$$

$$P_b(t) = P_b^{chp}(t) + P_b^r(t) + P_b^{dis}(t) + P_b^{gimp}(t) - P_b^{ch}(t) - P_b^{gexp}(t). \tag{5.9}$$

Here, $P_b(t)$ is the total demand of b-th building, $P_b^{chp}(t)$ is the electric output power of CHP generator, $P_b^r(t)$ is the renewable power generation of b-th smart building, $P_b^{ch}(t)$ and $P_b^{dis}(t)$ are respectively the battery charging and discharging power of b-th SB. $P_b^{gimp}(t)$ and $P_b^{gexp}(t)$ are the grid import and export powers of b-th SB.

The total renewable power from solar PV and wind turbine is calculated as,

$$P_b^r(t) = P_b^s(t) + P_b^w(t), \tag{5.10}$$

where, P^s and P^w are respectively the solar PV power and wind turbine power which are described in Chapter 2.

The power balance equation incorporating power trading between SBs is given by the following equation.

$$\begin{aligned} P_b(t) = P_b^{chp}(t) + PR_b(t) + P_b^{dis}(t) + P_b^{gimp}(t) - P_b^{ch}(t) - P_b^{gexp}(t) \\ + \sum_{n,b\neq n} P_{bim}(b,n,t) - \sum_{n,b\neq n} P_{bex}(b,n,t), \end{aligned} \tag{5.11}$$

where, $P_{bim}(b,n,t)$ is the import power from the n^{th} SB at time t and $P_{bex}(b,n,t)$ is the export power to the n^{th} SB.

The total power consumption of each SB during any interval should not exceed the MDL defined by the grid. This constraint can be formulated as follows,

$$P_b(t) \leq P_{mdl}, \tag{5.12}$$

where, P_{mdl} is the Maximum Demand Limit (MDL) defined by the utility.

CHP generators are subject to their rating for generating electric power output as given bellow.

$$P_b^{chp}(t) \leq P_c^{chp}, \tag{5.13}$$

where, P_c^{chp} is the rated capacity of CHP generator. Total heat generated from the CHP generator can be described by the following equation,

$$H_b^{chp}(t) = \frac{P_b^{chp}(t)}{PR}, \tag{5.14}$$

where, $H_b^{chp}(t)$ is the total heat generated from CHP generator and PR is the power ratio of CHP generator.

Temperature Dependent Loads (TDLs) operate in a particular range of temperatures described as follows,

$$T_{a_{td}}^{min} \leq T_{a_{td}}(t) \leq T_{a_{td}}^{max}, \tag{5.15}$$

where, $T_{a_{td}}(t)$ is known as operating temperature of the TDLs at time interval t, and $T_{a_{td}}^{min}$ and $T_{a_{td}}^{max}$ are the minimum and maximum operating limits of the TDLs.

Battery storage system is constrained by specific parameters, i.e., battery capacity, maximum charging-discharging rating, State-of-Charge (SOC) limits. Available SOC of the battery at time interval $t+1$ is depends on the SOC, charging/discharging power at time interval t, and charging/discharging efficiency and can be expressed as follows.

$$SOC_{(t+1),b} = SOC_{t,b} \times (1-\sigma) + (P_b^{ch}(t)\eta^{ch} - P_b^{dis}(t)/\eta^{dis}), \tag{5.16}$$

The SOC of BSS should be maintained within its maximum and minimum limits of SOC^{max} and SOC^{min} respectively.

$$SOC^{min} \leq SOC_b(t) \leq SOC^{max}. \tag{5.17}$$

Battery can't charge and discharge simultaneously, i.e.,

$$P_b^{ch}(t) \leq \alpha_{1,b}(t) \times P_{max,b}^{ch}(t), \tag{5.18}$$

and

$$P_b^{dis}(t) \leq (1-\alpha_{1,b}(t)) \times P_{max,b}^{dis}(t), \tag{5.19}$$

where, $\alpha_{1,b}$ is battery binary variable of b^{th} SB. When battery is charging at a given time interval t, then $\alpha_{1,b} = 1$ and it is 0 when the battery is discharging.
Charging and discharging power of battery are constrained as follows,

$$\eta^{ch} P_b^{ch}(t) \leq min\left(P_b^{ch,max}(t), \left(\frac{BC}{100}\Big(SOC^{max} - SOC_{(t-1),b}\Big)\right)\right), \tag{5.20}$$

and

$$\frac{P_b^{dis}(t)}{\eta^{dis}} \leq min\left(P_b^{dis,max}(t), \left(\frac{BC}{100}\Big(SOC_{(t-1),b} - SOC^{min}\Big)\right)\right), \tag{5.21}$$

where, BC is the battery capacity.

The Thermal Storage System (TSS) has been described below in similar terms as described for BSSs above. Available SOC of TSS is obtained from the following expression.

$$SOC^T(t+1,b) = SOC^T(t,b) + \eta^{chT} \times P^{chT}(b,t) - P^{disT}(b,t)/\eta^{disT} \tag{5.22}$$

The SOC of TSS cannot violate its maximum and minimum SOC limits i.e., $SOC^{T,max}$ and $SOC^{T,min}$ respectively,

$$SOC^{T,min} \leq SOC^T(t,b) \leq SOC^{T,max}, \tag{5.23}$$

and simultaneous charge and discharge of TSS are prohibited i.e.,

$$P^{disT}(b,t) \leq (1 - \alpha_2(b,t)) \times P_{max}^{disT}(b), \tag{5.24}$$

and

$$P^{chT}(b,t) \leq \alpha_2(b,t) \times P_{max}^{chT}(b). \tag{5.25}$$

In the above equations, SOC^T is the SOC of TSS, $P^{chT}(b,t)$ and $P^{disT}(b,t)$ are respectively TSS charging and discharging power for b^{th} smart building at time t, $\alpha_2(b,t)$ is the binary variable of TSS for b^{th} smart building.

Buying and selling of power to/from the utility grid is not possible at the same time and can be specified using the following equations,

$$P_b^{gimp}(t) \leq \alpha_b(t) \times P_b^{gimp,max}, \tag{5.26}$$

and

$$P_b^{gexp}(t) \leq P_b^{gexp,max} \times (1 - \alpha_b(t)), \tag{5.27}$$

where, α_b is binary variable which indicates the import/export status of the b^{th} SB, $P_b^{gimp,max}$ and $P_b^{gexp,max}$ are the maximum import and export power limit from the grid.

Similarly, an SB cannot simultaneously import and export electricity from other SBs, i.e.,

$$P_{\substack{bim \\ b \neq n}}(b,n,t) = P_{bim}^{max} \times \alpha_{ex}(b,t), \tag{5.28}$$

$$P_{\substack{bex \\ b \neq n}}(b,n,t) = P_{bex}^{max} \times (1 - \alpha_{ex}(b,t)), \tag{5.29}$$

where, P_{bim}^{max} and P_{bex}^{max} are the maximum import and export power limit among the SBs, and $\alpha_{ex}(b,t)$ is the binary variable of b^{th} SB at time interval t.

The total heat demand of b^{th} SB is calculated as,

$$H^{d}(b,t) = H_{b}^{chp}(t) + H^{disT}(b,t) - H^{chT}(b,t), \tag{5.30}$$

$$H^{disT}(b,t) = \frac{P^{disT}(b,t)}{\eta^{disT}}, \tag{5.31}$$

and

$$H^{chT}(b,t) = \frac{P^{chT}(b,t)}{\eta^{chT}}, \tag{5.32}$$

where, $H^{d}(b,t)$ is the total heat demand of the b^{th} smart building, $H^{disT}(b,t)$ and $H^{chT}(b,t)$ are respectively total discharging and charging heat of TSS. η^{disT} and η^{chT} are discharging and charging efficiency of TSS respectively.

5.3.2 Price and Bill Prediction

For prediction of the electricity price a GPR(Gaussian process Regression) model is developed. The different types of data set used in developing the model are as follows.

Training data set-: Training data set is used to train the model.

Testing data set-: Testing data set is used to check the model performance, that is when testing data given to the trained model, it predicts the output. Then we have calculated performance metrics by comparing the predicted data and actual data.

Cross validation data -: Cross validation data is used for hyper-parameter tuning of the model during the training period. Therefore 5-10% data of training data set is used for cross validation.

To forecast price data, three months of historical time series price data have been considered. The GPR machine learning model has been considered here for price forecasting. To find the accuracy of the GPR model, we have calculated different performance parameters such as Root Mean Square Error (RMSE), R-squared, Mean Squared Error (MSE) and Mean Absolute Error (MAE). The performance parameters has been calculated considering the actual data and the predicted data. The performance of different combinations of training and testing data set is shown in the Table 5.1. The accuracy of FDI attack detection depends on the accuracy of the forecasted price. In the case of FDI attack detection, the scheduling is performed considering the forecasted price rather

than the price received from the smart meter. Therefore, the accuracy of forecasts affects both the detection of FDI attacks and the energy cost for buildings. From the Table 5.1, we found that 60-40% combination gives the highest accuracy among the considered combinations. Therefore, we have considered 60% data set for training and 40% data set for testing of the total data set in our work. A validation set of 10% of training data has been used for model validation. To prevent model over fitting, L2 regularization has been adopted. Optimal hyper-parameters were chosen, on the basis of minimization of the Root Mean Square Error (RMSE) loss function. A sample 24 hour ahead forecast of price data is given in Table 5.2. Figure 5.2 shows the details of price forecasting based on machine leaning regression model. The demand is scheduled using forecasted price and the reference bill is generated using Eq. 5.2.

Table 5.1: Performance table on different training and testing data

Sl.No	Cases (training, testing data)	RMSE	R-squared	MSE	MAE
01	case-1(60, 40)	0.12	0.93	0.01	0.10
02	case-2(50, 50)	0.19	0.85	0.04	0.14
03	case-3(40,60)	0.26	0.67	0.07	0.17

5.3.3 FDI Attack Detection and Defense Strategy

The price defined by the utility is prone to FDI attack by the attacker. The attacker can change the utility's price by injecting some positive or negative value into the actual price. It is difficult for the user to estimate the actual change in the utility price by an attacker. Users can reduce the impact of FDI attack on their scheduling to a certain level. In general, a particular residential user follows a similar pattern of daily load demand. Also, the price of electricity may vary, but the shape of the price curve is roughly the same as for the previous days' shape. The information of these tendencies can be used to detect FDI attack. In this work, electricity price is forecasted based on data from the previous 90 days using machine learning. The predicted bill B^R, consumption pattern $P_b^R(t)$, import and export powers based on forecasted price are used as a reference. The scheduling obtained based on reference data and scheduling obtained based on the actual

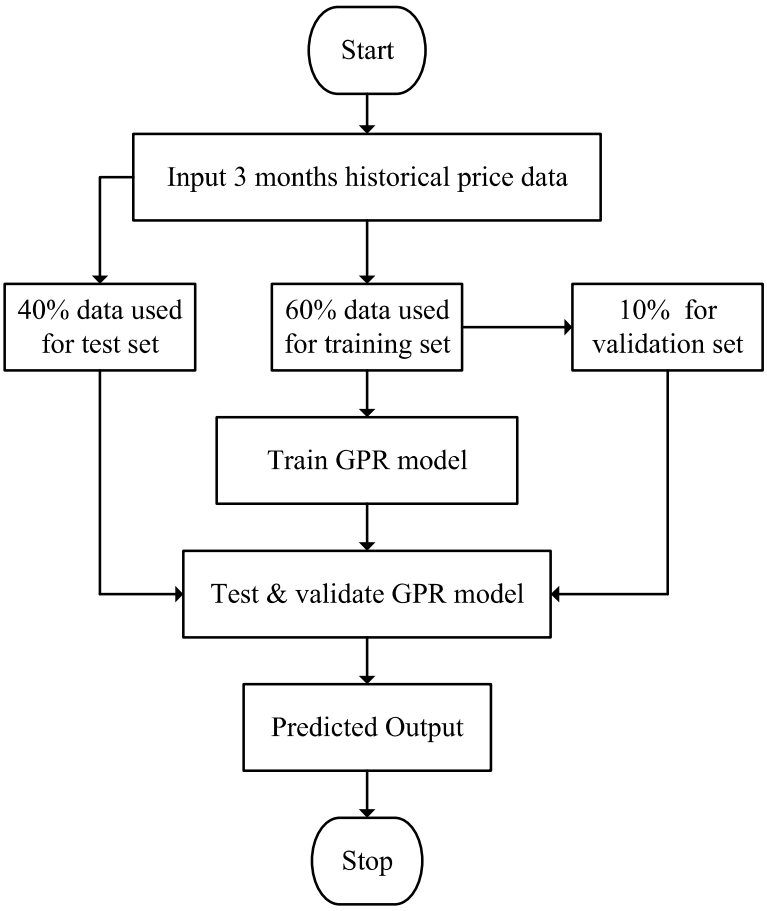

Figure 5.2: flowchart depicting method of price forecasting

data are compared. If B and $P_b(t)$ are the bill and demand based on actual price data, the per unit (PU) bill increase/decrease, ΔB, can be calculated as,

$$\Delta B = \frac{B - B^R}{B^R}. \tag{5.33}$$

The maximum change in demand can be calculated as

$$\Delta P(t) = (P_b(t) - P_b^R(t))/P_b^R(t). \tag{5.34}$$

These two changes, $|\Delta B|$ and $|\Delta P|$, are compared with tolerance limits δb and δp respectively. If $|\Delta B| > \delta b$, or $|\Delta P| > \delta p$, then a possible false data injection attack in the price data is flagged. In such a case, the following constraints are used for the resilient scheduling.

$$0.9P_b^{imp,R}(t) \leq \left(P_b^{gimp}(t) + \sum_n \sum_{b \neq n} P_{bim}(b, n, t)\right) \leq 1.1P_b^{imp,R}(t) \tag{5.35}$$

$$0.9P_b^{exp,R}(t) \leq \left(P_b^{gexp}(t) + \sum_{\substack{n \\ b \neq n}} P_{bex}(b,n,t)\right) \leq 1.1P_b^{exp,R}(t) \tag{5.36}$$

$P_b^{imp,R}(t)$ and $P_b^{exp,R}(t)$ are respectively the total reference import and export power of b^{th} smart building at t^{th} time interval. Eq. 5.35 and Eq. 5.36 are used to capture users' past behaviour. The complete detection mechanism is given in the flowchart of Figure 5.3.

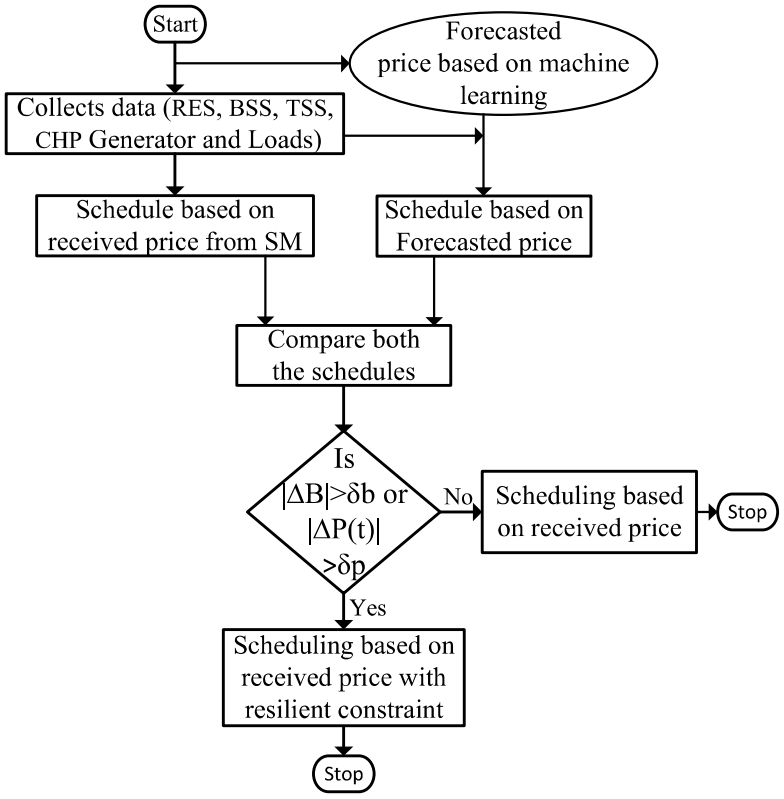

Figure 5.3: Flowchart Depicting the Detection Strategy

5.4 Results and Discussion

The proposed MSBEMS is validated on a system having different SH appliances (loads), DERs, and CHP generators. Different types of SH appliances, viz. refrigerator, TV, laptop, fluorescent lamp, washing machine, dish washer, tumble dryer, cooker oven, vacuum cleaner, electric vehicle, along with their ratings are given in Table 5.3. Battery storage capacity of 10 kWh and thermal storage capacity of 20 kWh are installed at each SB. CHP generator is installed at each SB with specifications as depicted in Table 5.4. The specifications of the Renewable Energy Sources (RESs) are depicted in Table 5.5. The

Table 5.3: Appliances Specification

Sl.No	Name of Appliances	$P_{rated}(kW)$	Length of Operation (Hour)
1	Laptop	0.1	2
2	Refrigerator	0.3	24
3	Fluorescent Lamp	0.84	6
4	TV	0.3	3
5	Washing Machine	2.1	2
6	Dish Washer	2.1	2
7	Tumble Dryer	4	2
8	Cooker Hob	3	1
9	Microwave	1.7	1
10	Cooker Oven	5	1
11	Vaccum Cleaner	1.2	1
12	Electric Vehicle	3.5	3

hourly forecasted price generated from the GPR model and actual price are shown in Table 5.2. The renewable energy generated from solar and wind are depicted in Figure 5.4. The natural gas price, λ_g, and battery maintenance cost, λ_{bmc}, are considered as 2.7 ₹/kWh and 0.5 ₹/kWh respectively. The MDL is considered as 15kW for each SB. The proposed Mixed Integer Programming (MIP) framework is implemented in General Algebraic Model System (GAMS), and CPLEX solver is used to solve the problem.

Table 5.2: Forecasted and Received Price

Time (Hour)	1	2	3	4	5	6	7	8	9	10	11	12	13	14	15	16	17	18	19	20	21	22	23	24
Forecasted Price(₹)	2.9	2.7	3	3	1.8	3	3.75	3.5	3.2	3	3.1	3.15	2.8	2.7	2.65	2.75	3	4.25	3.5	3.15	2.9	2.9	2.6	2.6
Recived Price(₹)	2.9	2.7	3	3	3.5	3	2.5	2.75	3.2	3	3.1	3.15	2.8	3	3.5	4	3.25	3	2.75	3	2.9	2.9	2.6	2.6

Table 5.4: CHP Generator specification.

SB	Capacity (kW)	efficiency	Power Ratio
1	20	35	1.3
2	20	40	1.2
3	40	35	1.3

Table 5.5: Renewable Energy Resources Specification.

Sl.No	Components	Rating	Count	Total rating
1	Solar PV	0.1 kw	24	2.4 kW
2	Wind turbine	1 kw	2	2 kW

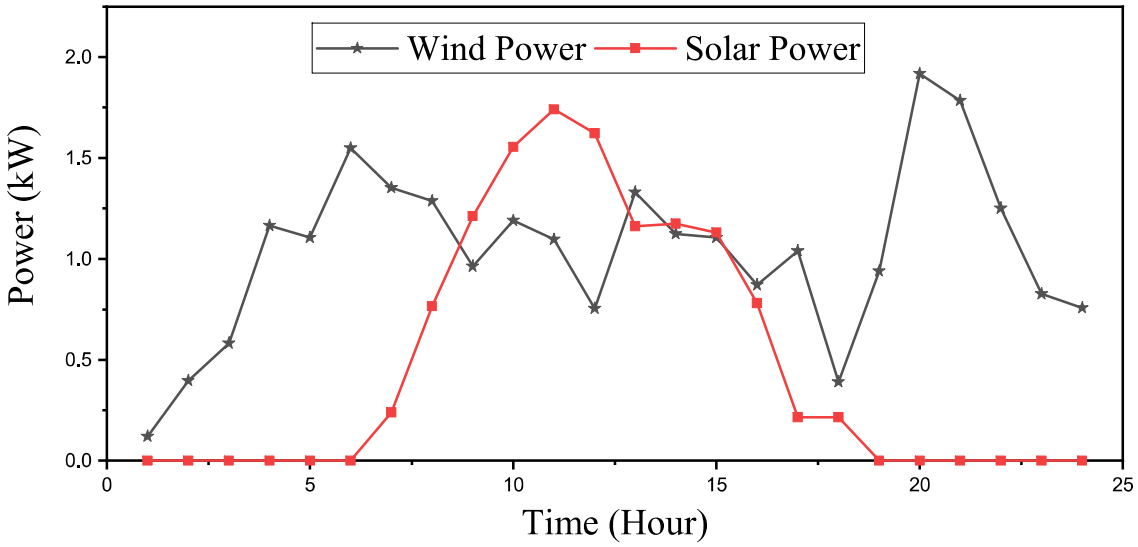

Figure 5.4: RES Generation

5.4.1 Energy Cost Minimization with and without Power Exchange among Smart Buildings

Two cases are considered in this section, i.e., scheduling without inter-SB power exchange ($CaseI$) and scheduling with inter-SB power exchange ($CaseII$). Scheduled demands with and without power exchange between SBs are shown in Figure 5.5.

It is observed that each SB tries to schedule higher load during a low tariff period

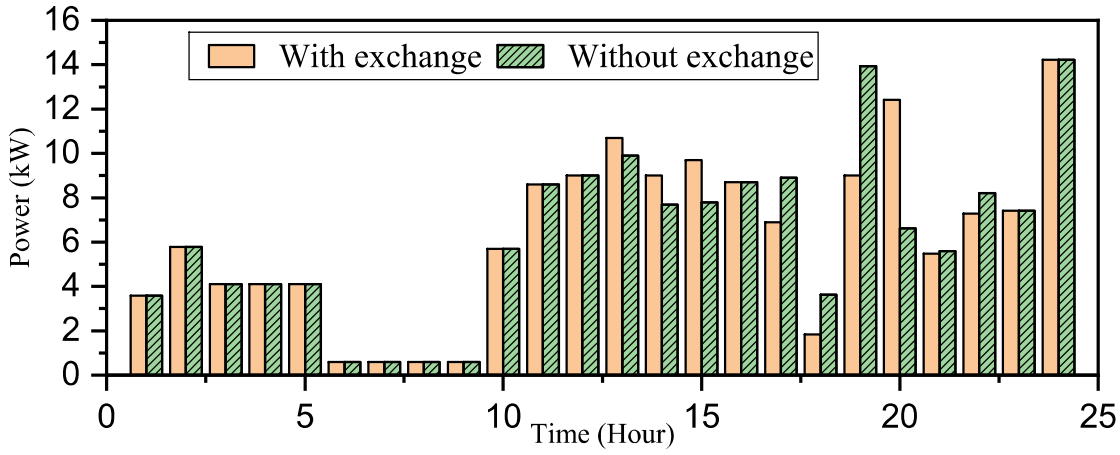

(a) SB1

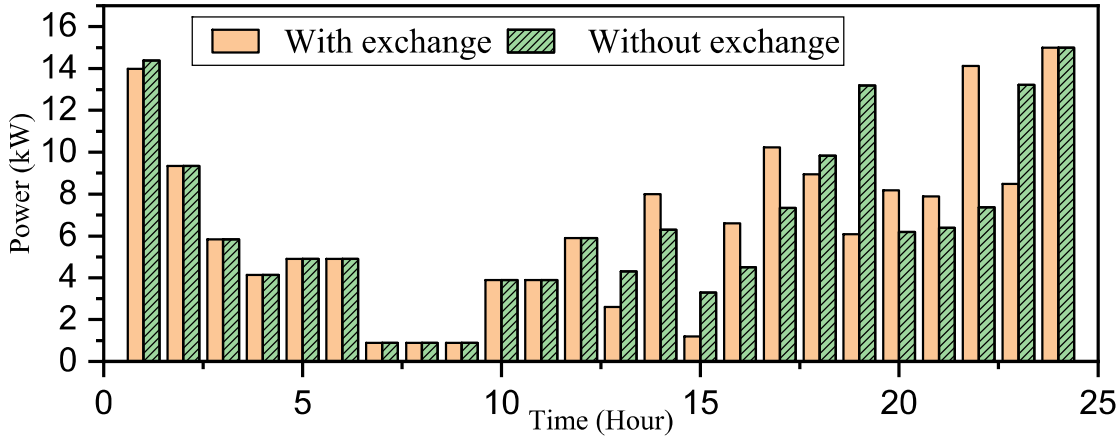

(b) SB2

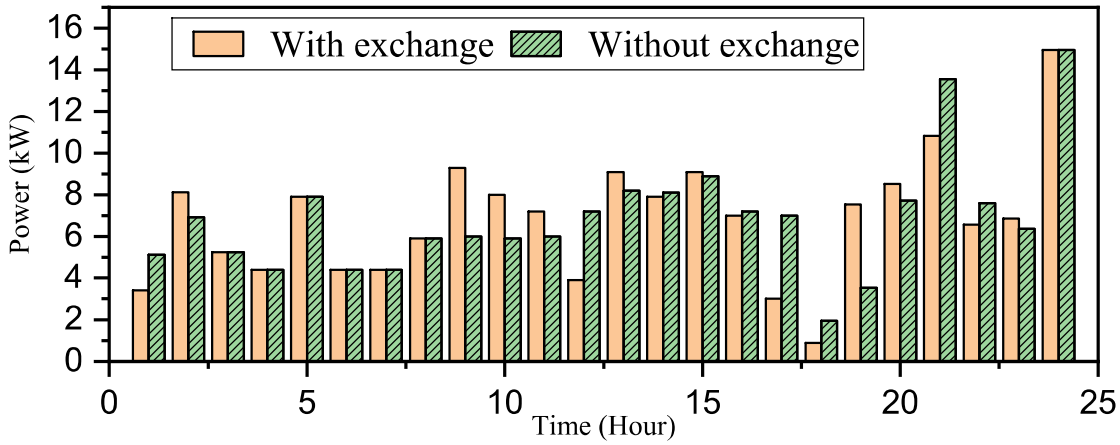

(c) SB3

Figure 5.5: Scheduled demand with and without power exchange

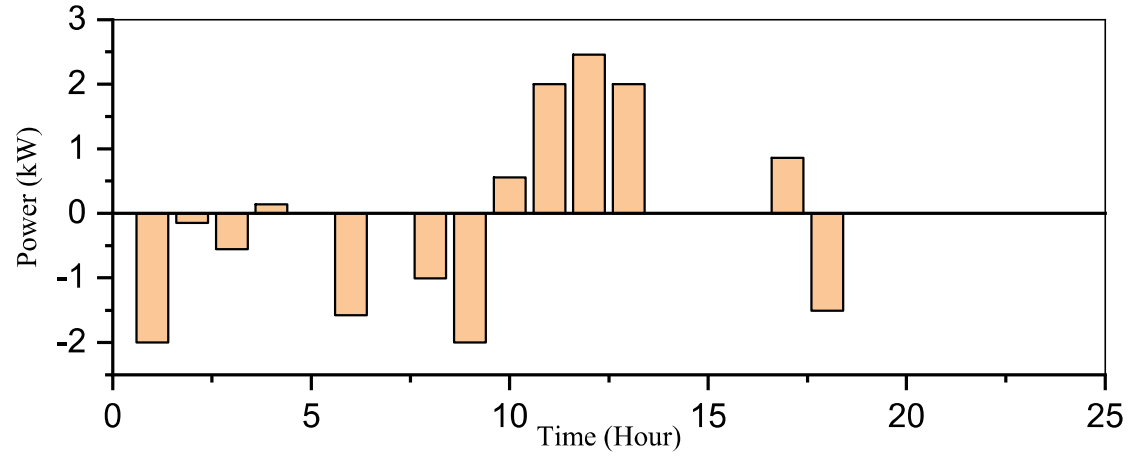

(a) SB1

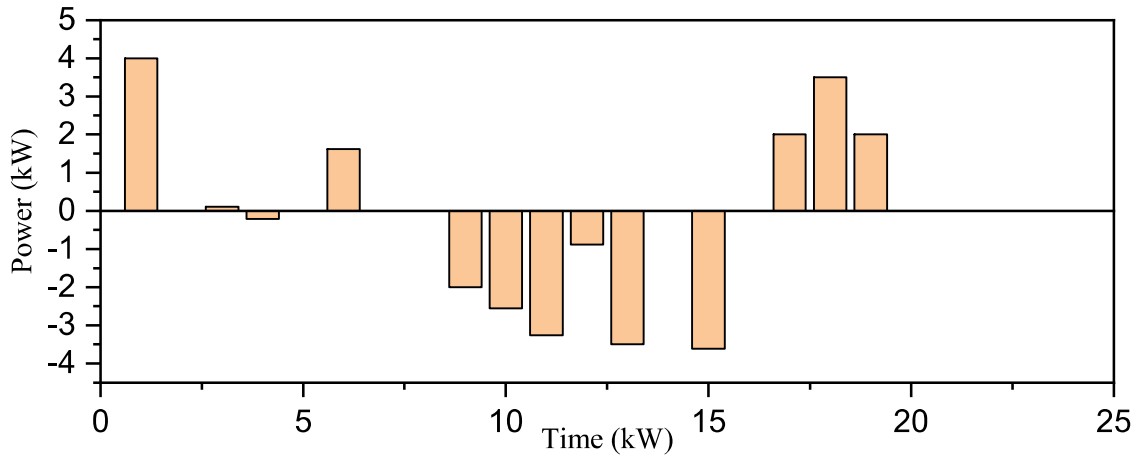

(b) SB2

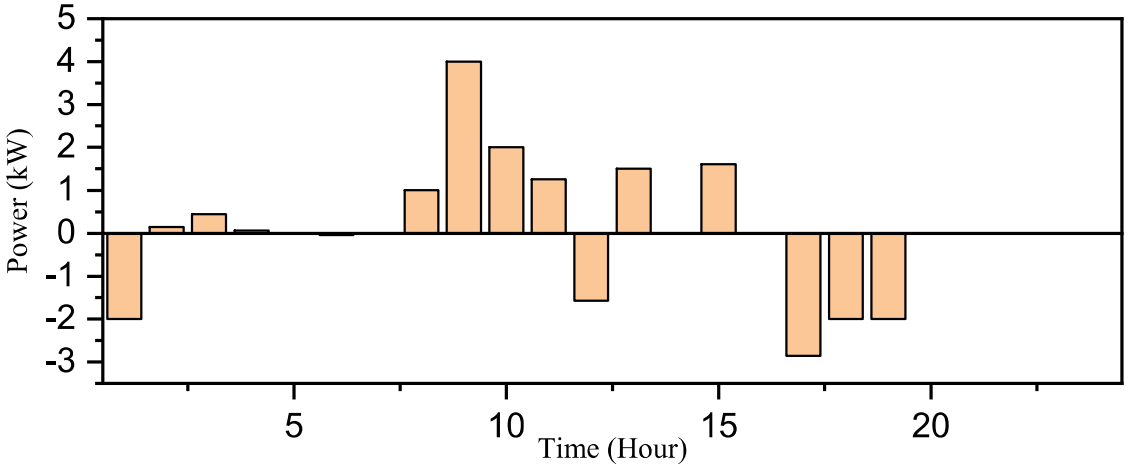

(c) SB3

Figure 5.6: Inter-Smart Building Power Exchange

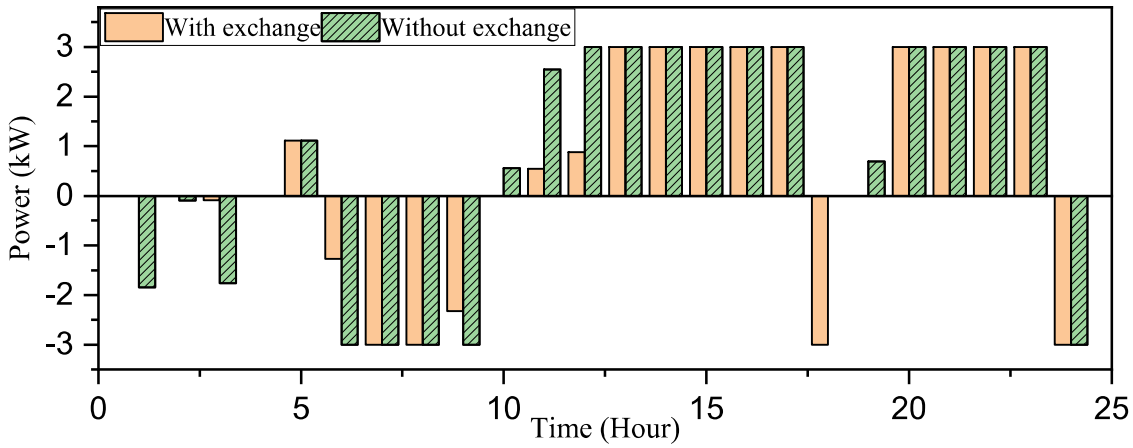

(a) SB1

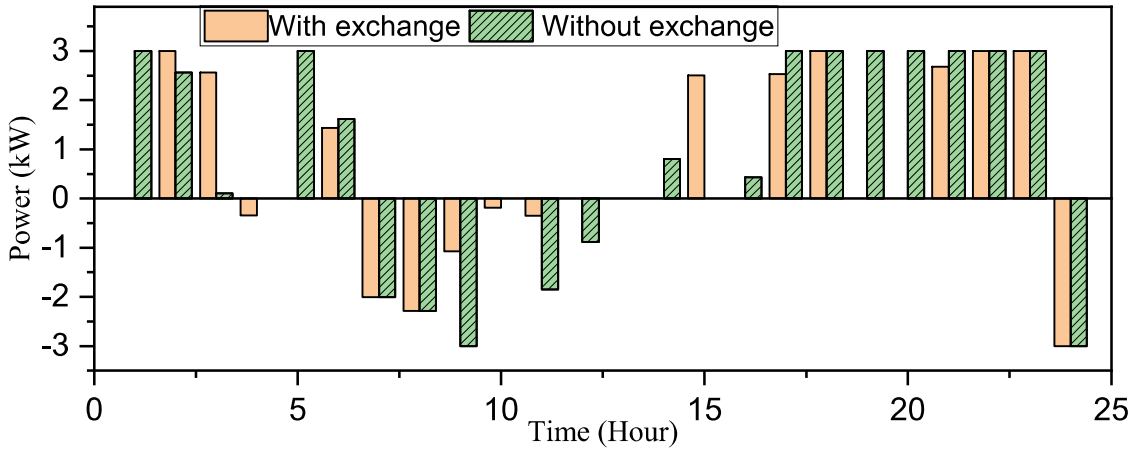

(b) SB2

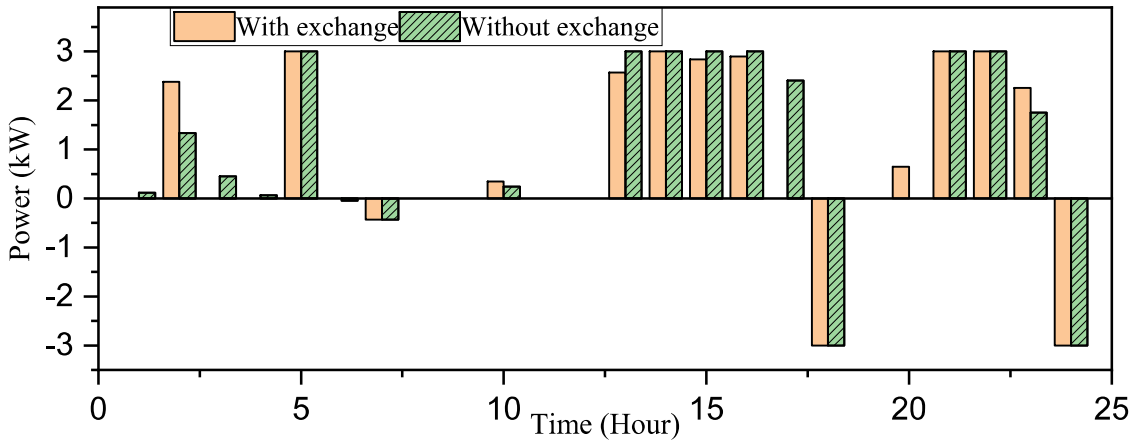

(c) SB3

Figure 5.7: Grid Exchange Power

Table 5.6: Energy Cost

SBs	Without exchange(₹)	With exchange (₹)	Reduction (%)
1	228.68	215.489	5.76
2	257.67	240.487	6.66
3	250.406	247.358	1.21
Total cost	736.7557	703.334	4.53

or during a high RES generation period. The SB operator would avoid purchasing power from the grid during high price periods (7:00–9:00 hours and 18:00–19:00 hours; Table 5.2), as shown in the Figure 5.5, where a higher demand is scheduled during 18:00–19:00 hours in $CaseI$ than in the $CaseII$. In $CaseI$ SB1 tries to import more power during the low price period (13:00–15:00 hours), but due to the limits imposed on maximum imports from the grid, SB1 needs to transfer some of the load in the higher price period (17:00–19:00 hours). It is observed from Figure 5.6 that SB1 imports power from both grid and SB2 (in $CaseII$) during 13:00–15:00 hours, this happen due to the fact that during 13:00–15:00 hours SB2 has surplus RES generation. The inter-SB power exchange price is assumed to be the same as SB to grid export price. Therefore, the seller SB receives same revenue either it sells energy to grid or other SBs. But, buyer SB can purchase energy at a low cost from other SBs as compared to grid. It is observed from Figure 5.6 and Figure 5.7, SB2 reduces the export power to grid in $CaseII$ (as compared to $CaseI$) during 13:00–15:00 hours but increases power export to SB1. It has been observed that, when power exchange capability is considered, the total power import/export to the grid is less than the power import/export without considering the power exchange capability. The power exchange between the buildings results decrease in power import /export from/to the grid due to maximum utilization of renewable energy generation among the SBs.

The energy cost with inter-SB power exchange is less as compared to energy cost without inter-SB power exchange, as depicted in Table 5.6. It is found that the total energy cost for a particular day without inter-SB power exchange is ₹736.7557 whereas it is ₹703.334 with inter-SB power exchange. It can be concluded that the inter-SB power exchange in MSBEMS reduces the total electricity bill for a particular day by using the diversity of consumer demand in SBs.

5.4.2 Analysis of FDI Attack Detection and Defense Strategy

This section describes the effectiveness of detection of FDI attack and resilience in scheduling. Table 5.7 depicts the energy cost and change of energy cost (%) for each of the SBs under different cases. As shown in the Table 5.7, the values of ΔB are very large, i.e., 56.41%, 32.04%, and 34.05% for SB1, SB2, and SB3 respectively, but in real life, there is no sudden change in consumer behavior or utility price. This change in energy costs reflects some malicious activity, i.e., FDI attack in utility price. From the given Table 5.7, it is noticed that energy cost with resilient scheduling is nearly equal to the energy cost with reference scheduling. The total energy cost with scheduling resilient against FDI attack is ₹731.196, while it is ₹703.334 without attack.

Figure 5.8 shows scheduled demand patterns with and without FDI attack, and with resilient scheduling . It is observed that FDI attack on price data can shift scheduled demand peak and valley. This shifting may increase consumers' energy cost. In resilient scheduling process, scheduling of SB appliances not only depend on utility price, but also depends on past consumer demand pattern. Figure 5.8 shows that for reference scheduling and resilient scheduling scheduled demand pattern do not differ significantly. The import/export power from/to the grid at different demand scheduling (without attack, with attack and with resilient scheduling) are shown in Figure 5.9. The Figure 5.9 shows that, the import and export power for the case of without attack and for the case of resilient scheduling are nearly similar to each other. The total import power for the case of without attack is 83.122 kW whereas, it is 93.166 kW in case of FDI attack with resilient scheduling which are nearly equal to each other.

Table 5.7: Energy cost under FDI attack and resilient scheduling against FDI attack

SBs	Cost with attack(B)	without attack cost (B^P)	ΔB in %	Cost with Resilient Scheduling
01	337.056	215.489	56.41	220.819
02	317.552	240.487	32.04	251.829
03	331.602	247.358	34.05	258.548
Total Cost	986.211	703.334	40.21	731.196

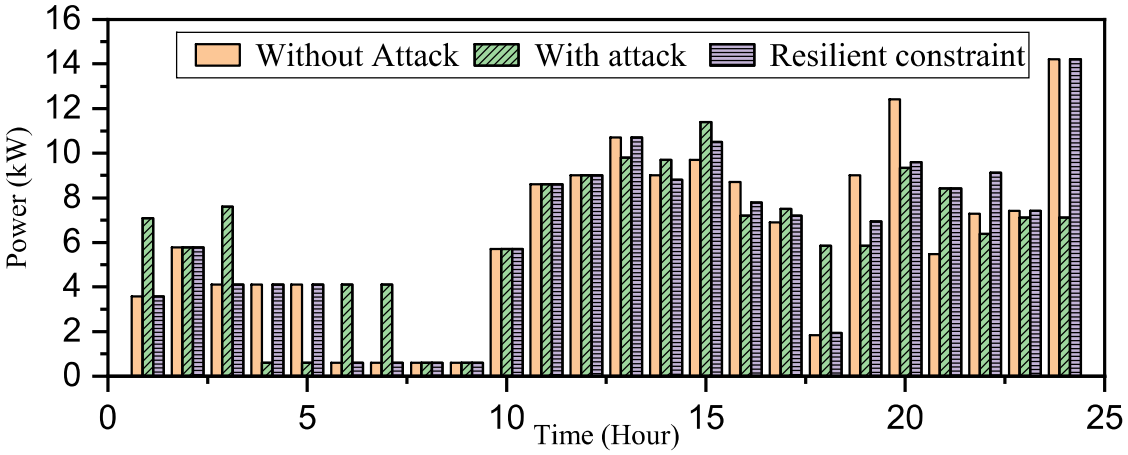

(a) SB1

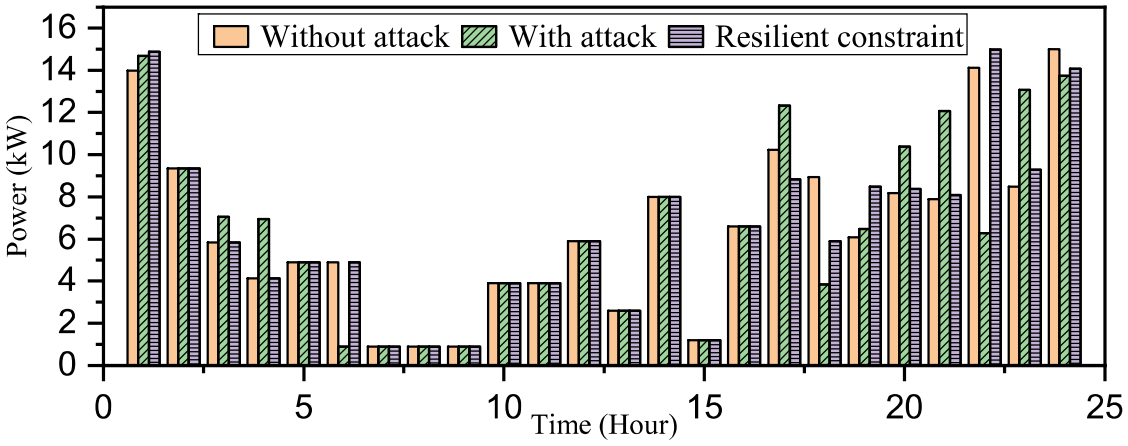

(b) SB2

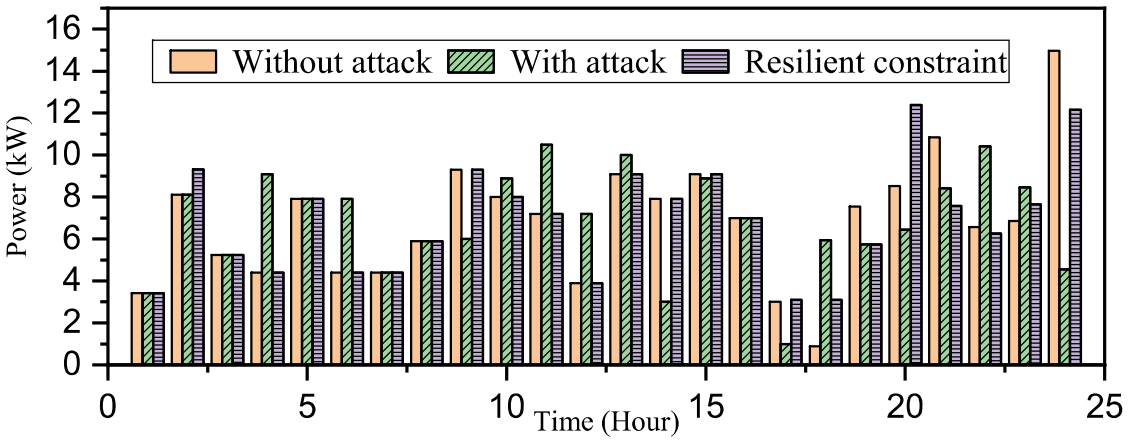

(c) SB3

Figure 5.8: Demand without attack, with attack and with resilient

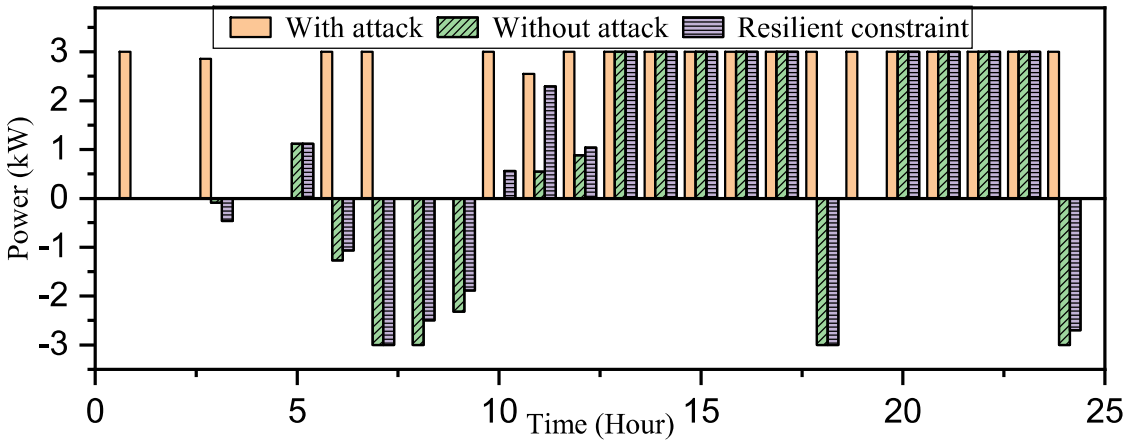

(a) SB1

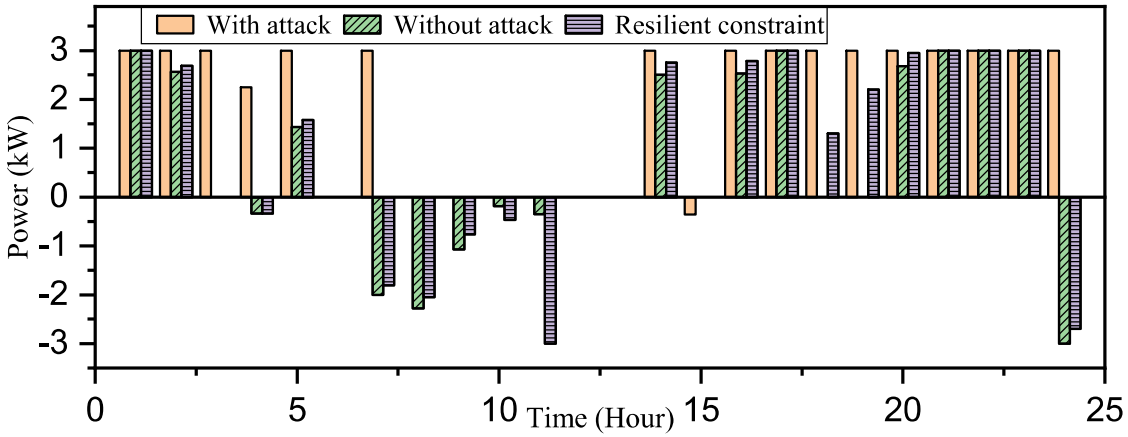

(b) SB2

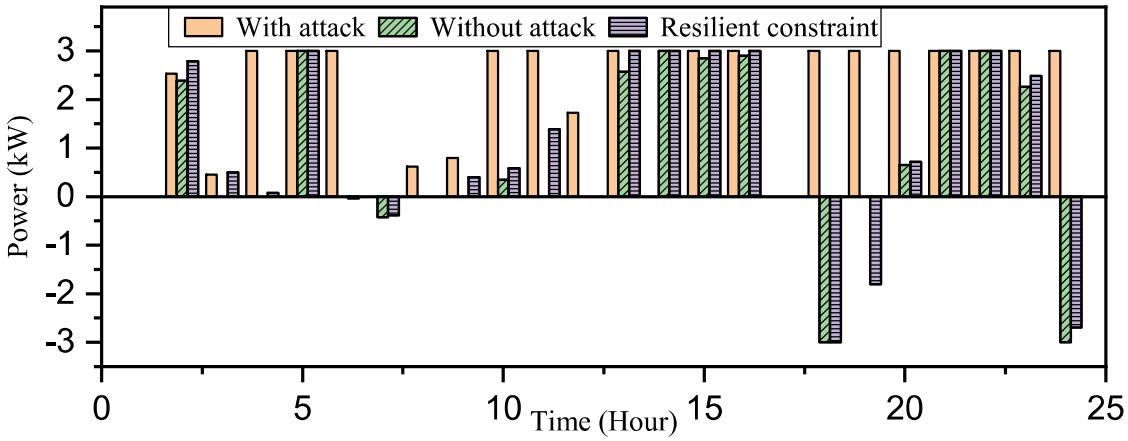

(c) SB3

Figure 5.9: Grid import and export power without attack, with attack and with resilient

However, the proposed method also has a boundary condition that can bypass the detection of FDI attacks. To find the boundary scenario, a sensitivity analysis considering different FDI attacks has been carried out. The result of the boundary condition is summarized in Table 5.8. The sensitivity analysis shows that the proposed FDI detection strategy fails to detect the FDI attack below $GN(0,0.13)$ due to a small changes in bill and demand.

Table 5.8: Sensitivity Analysis

Sl. No	FDI Attack	Proposed Method			Existing Method [108]
		$\|\Delta B\| > \delta b$	$\|\Delta P\| > \delta p$	Detection	Detection
01	$GN(0,0.01)$	7.1×10^{-6}>0.05 (No)	.36>.4 (No)	No	No
02	$GN(0,0.02)$	1.27×10^{-5}>0.05 (No)	.302>.4 (No)	No	No
03	$GN(0,0.03)$	1.84×10^{-5}>0.05 (No)	.325>.4 (No)	No	No
04	$GN(0,0.04)$	2.41×10^{-5}>0.05 (No)	.254>.4 (No)	No	No
05	$GN(0,0.05)$	2.98×10^{-5}>0.05 (No)	.256>.4 (No)	No	No
06	$GN(0,0.06)$	$3.69\times^{-5}$>0.05 (No)	0.265>.4 (No)	No	No
07	$GN(0,0.07)$	$5.68\times^{-5}$>0.05 (No)	0.376>.4 (No)	No	No
08	$GN(0,0.08)$	$5.4\times^{-5}$>0.05 (No)	0.272>.4 (No)	No	No
09	$GN(0,0.09)$	7.1×10^{-5}>0.05 (No)	.282>.4 (No)	No	No
10	$GN(0,0.1)$	$8.67\times^{-5}$>0.05 (No)	0.281>.4 (No)	No	No
11	$GN(0,0.11)$	0.0001>0.05 (No)	0.277>.4 (No)	No	No
12	$GN(0,0.12)$	0.00012>0.05 (No)	0.175>.4 (No)	No	No
13	$GN(0,0.13)$	0.00015>0.05 (No)	0.593>.4 (Yes)	Yes	No
14	$GN(0,0.14)$	0.00018>0.05 (No)	0.593>.4 (Yes)	Yes	No
15	$GN(0,0.15)$	0.00021>0.05 (No)	0.593>.4 (Yes)	Yes	Yes
16	$GN(0,0.16)$	0.00024>0.05 (No)	0.593>.4 (Yes)	Yes	Yes
17	$GN(0,0.17)$	0.00027>0.05 (No)	0.593>.4 (Yes)	Yes	Yes
18	$GN(0,0.18)$	0.0003>0.05 (No)	1.007>.4 (Yes)	Yes	Yes
19	$GN(0,0.19)$	0.00033>0.05 (No)	0.593>.4 (Yes)	Yes	Yes
20	$GN(0,0.2)$	0.00036>0.05 (No)	0.705>.4 (Yes)	Yes	Yes

A cyber-attack detection technique, which is an anomaly detection method, is proposed in [96]. It states that if $|B-M| > kV$, a false data probably exists. Where, M and V represent the mean and standard deviation of the total bill of all buildings, respectively. k is a user defined threshold parameter which is considered as 0.5 [96]. In the present work, the values of M and V are estimated at 705 and 40, respectively. Following two different FDI attacks are considered for comparison of proposed detection technique with anomaly detection method [96]. (i) Case-a: FDI attack on price signal as shown in Table 5.2. (ii) Case-b: FDI attack with Gaussian Noise $GN(0,0.75)$. The total bill in case-a and case-b are ₹986.211 and ₹701.048, respectively. In case-a both the methods detect the FDI attack. The existing method is unable to detect the FDI attack in case-b because $|B-M| > kV$ is not satisfied. Also, the value of ΔB in the proposed method is too small to detect the attack. But the power demand constraint ΔP detects the attack in proposed method. The performance of proposed and existing method is summarized in Table 5.9.

Table 5.9: Comparison Between Anomaly Method and Proposed Method

FDI Attack	Anomaly Method [96]		Proposed Method		
	$\|B-M\| > kV$	Detection	$\|\Delta B\| > \delta b$	$\|\Delta P\| > \delta p$	Detection
Attacked price (Table 5.2)	281.211>20 (Yes)	Yes	40.21>5 (Yes)	.593>.4 (Yes)	Yes
Attack with $GN(0,0.75)$	3.952>20 (No)	No	0.32 >5 (No)	.593 >.4 (Yes)	Yes

Authors in [108], have proposed a short-term detection technique considering the pricing cyber-attack in smart home energy management system. Existing short-term detection techniques [108] have used a Binary Logistic Regression (BLR) engine to determines the cyber-attack. According to this method, smart home appliances (load) are scheduled based on the forecasted price signal to find the forecasted demand profile. Similarly, smart home loads are rescheduled based on attack price signals to find anomalous load profile patterns. Subsequently, both data sources are fed into the Binary Logistic Regression engine and are compared for detection of anomalies.

Mathematically, BLR takes N independent training samples, in which each sample

contains a covariate vector of length p. In our work, the samples consist of both forecasted demand profile and the attacked demand profile. Such profile are denoted as, x_i, and given as follows,

$$x_i = (x_1, x_2, x_3, ..., x_p)^T$$

where, x_i represents as sample i, in which x_p indicates the 24-Hour demand profile of consumer ending at time slot p. Similarly, y_i denotes the binary response which indicates that whether the cyber-attacks are present or not, which is described as follows,

$$y_i = \begin{cases} 1, & \text{anomalies} \\ 0, & \text{no anomalies.} \end{cases} \tag{5.37}$$

The target of BLR is to find the set of parameters as β_0 and $\beta = \{\beta_1, \beta_2, ..., \beta_p\}$ such that the model accurately determines the probability that the consumer is associated with cyber-attacks. The probability can be expressed in terms of β and x_i as the logistic function given in (5.38)

$$\pi_i = P(y_i = 1|x_i) = \frac{1}{1 + e^{-(\beta_0 + \beta_1 x_1 + \beta_2 x_2 + ... + \beta_p x_p)}} \tag{5.38}$$

The parameter set β is optimized through Maximum Likelihood Estimation (MLE), which attempts to maximize the likelihood function as follows,

$$L(\beta) = \prod_{i=1}^{N} \frac{e^{y_i(\beta_0 + \beta_1 x_1 + \beta_2 x_2 + ... + \beta_p x_p)}}{1 + e^{\beta_0 + \beta_1 x_1 + \beta_2 x_2 + ... + \beta_p x_p}} \tag{5.39}$$

where, y_i is the binomial count of the population group to which load profile x_i belongs. By solving the Eq.(5.39), we have obtained the β_0, and β values which are given in the Table 5.10.

Table 5.10: Estimated β values

Time	1	2	3	4	5	6	7	8	9	10	11	12	13	14	15	16	17	18	19	20	21	22	23	24
β	0	0	-1.382	-10.642	0	0	-6.986	0	0	-6.41	6.267	1.611	-11.607	-0.021	6.242	9.372	-6.232	-7.811	0	4.69	10.132	-3.455	2.374	0

For both cases, cyber-attack is reported if Eq. (5.40) holds.

$$\frac{1}{1 + e^{-(\beta_0 + \beta_1 . x_{t,1} + \beta_2 . x_{t,2} + ... + \beta_p . x_{t,p})}} \geq \pi_m \tag{5.40}$$

Similarly, for the both cases, cyber attack is not reported if Eq. (5.41) holds.

$$\frac{1}{1 + e^{-(\beta_0 + \beta_1 . x_{t,1} + \beta_2 . x_{t,2} + ... + \beta_p . x_{t,p})}} < \pi_m \tag{5.41}$$

Where, $x_t = \{x_{t,1}, x_{t,2}, ...x_{t,p}\}$ is the latest load profile and π_m is the minimum probability threshold for determining whether the load usage profile is anomalous. The calculated Probabilities for with attack, without attack and resilient strategy are found as 1, $2.11527E-23$ and $8.193600E-5$, respectively. It shows that our method can detect FDI attack effectively and the proposed resilience scheduling provides the scheduled power nearly same as without attack. We have also tested with the existing detection method [108], for different FDI attacks given in Table 5.8 and it is found that below $GN(0, 0.15)$, the existing technique [108] unable to detect FDI attack.

In this chapter we have also studied the FDI attack on the demand data, and coordinated attack on price and demand data. Table 5.11 shows the electricity bills of consumers under different conditions such as without attack, attack on demand data, and coordinated attack on (demand and price) data. From Table 5.11, it is observed that the electricity bill without attack and bill with resilient scheduling (against FDI attack on demand data) are nearly equal to each other. Further, it is noticed that electricity bill without attack and resilient scheduling (against FDI attack on both price and demand data) are also nearly equal to each other which shows the efficacy of the proposed resilient scheduling on the system.

Table 5.11: Bills of attack on demand data and both (price and demand) data

SBs	Bill(₹) without attack	Bill(₹) with		Resilient scheduling Bill(₹)	
		Demand attack	Both (price & demand attack)	demand attack	both (price & demand attack)
1	215.489	205.015	299.382	209.307	223.029
2	240.487	232.135	296.6	241.008	253.912
3	247.358	243.633	372.134	242.149	254.74

5.5 A comparison of centralized/decentralized approaches

In centralized approach, power exchange between smart buildings are considered but power exchange capability is not considered in decentralized approach. Tariff structure is also different for these two approaches.

centralized approach(Chapter 5)

1. The EMU of each smart buildings are connected to main EMU.
2. The main EMU is considered as centralized controller as it manages the total energy of the MSBEMSs and checks whether it is possible to import or export electricity between buildings.
3. A central controller (main EMU) is used for energy exchange among buildings whereas the utility tariff is considered as fixed.
4. Electricity bill without considering FDI attack for SB1, SB2 and SB3 are ₹215.489, ₹240.487 and ₹247.358, respectively.
5. Electricity bill with considering FDI attack for SB1, SB2 and SB3 are ₹337.056, ₹317.552 and ₹331.602, respectively.
6. Electricity bill with considering resilient constraint for SB1, SB2 and SB3 are ₹220.819, ₹251.829 and ₹258.548, respectively.

Decentralized approach(Chapter 4)

1. The EMU of each smart buildings are not connected to main EMU rather these communicate directly to the grid.
2. The strategy of each building (each EMU) affects the energy tariff of grid as it depend on the total demand of the buildings.
3. A non-cooperative game theory based strategy is used for energy management among the buildings.
4. Electricity bill without considering FDI attack for SB1, SB2 and SB3 are ₹395.082, ₹410.006 and ₹429.209, respectively.
5. Electricity bill with considering FDI attack for SB1, SB2 and SB3 are ₹423.335, ₹427.864 and ₹457.320, respectively.
6. Electricity bill with considering resilient constraint for SB1, SB2 and SB3 are ₹396.52, ₹411.44 and ₹430.903, respectively.

5.6 Summary

An energy scheduling problem for interconnected SBs having inter-SB energy exchange capability has been formulated as a MILP problem. The energy cost minimization approach is resilient towards FDI attack is proposed and developed in this chapter. For the

studied sample system it has been observed that the proposed formulation successfully detects the FDI attack and accordingly performs resilient energy scheduling in event of attack. The detection algorithm in the proposed formulation uses an additional metric based on difference of forecasted and actual power which makes the proposed algorithm more sensitive towards FDI attack as compared to existing method based on anomaly detection. From the sample system studies it was observed that when the system is under attack the energy cost without resilient scheduling is ₹986.211 whereas, when resilient scheduling is performed the energy cost is ₹731.196, establishing the efficacy of the proposed formulation.